Pyrene-containing twistarene : twelve benzene rings fused in a row

Chen, Wangqiao; Li, Xinxiong; Long, Guankui; Li, Yongxin; Ganguly, Rakesh; Zhang, Mingtao; Aratani, Naoki; Yamada, Hiroko; Liu, Ming; Zhang, Qichun

2018

Chen, W., Li, X., Long, G., Li, Y., Ganguly, R., Zhang, M., ... Zhang, Q. (2018). Pyrene-containing twistarene : twelve benzene rings fused in a row. Angewandte Chemie International Edition, 57(41), 13555-13559. doi:10.1002/anie.201808779

https://hdl.handle.net/10356/144117

https://doi.org/10.1002/anie.201808779

Pyrene-Contained Twistarene: Twelve Benzene Rings Fused in One Row

Wangqiao Chen,[a],[b] #Xinxiong Li,[a] # Guankui Long,[c] Yongxin Li,[e] Rakesh Ganguly,[e] Mingtao Zhang,[c] Naoki Aratani,[d] Hiroko Yamada,[d] Ming Liu[b]* and Qichun Zhang*[a]

Abstract: *Success in obtaining high twistarenes with precise structures is very important because such an approach could provide a lot of useful information in fundamentally understanding the relationship between structures and physical properties/optoelectronic applications. In this research, by envisioning the advantages from a retro-Diels-Alder process (clean reaction) and the cross-conjugated nature of pyrene unit, we successfully prepared a novel large dodecatwistarene (**4**) for the first time. Its structure, confirmed by single crystal XRD analysis, indicates that **4** possesses a twisted angle (~ 30°) and two neighboring molecules in the crystal lattice are perpendicular to each other due to the twisted feature and the strong intermolecular CH–π interactions. However, its basic physicochemical properties suggest its instability in air due to its elevated HOMO energy level although NICS calculation confirms that pyrene units have poor contribution to the π-conjugation of the whole molecule.*

As one family member of graphene nanoribbons, arenes and their analogues have been demonstrated to show unique optoelectronic properties[1] and potential applications in organic field-effect transistors (OFETs),[2] organic light-emitting diodes (OLEDs),[3] and photovoltaic cells,[4] as well as in spintronics[5] and plasmonics.[6] These promising factors strongly encourage scientists to design and prepare novel larger homoanalogues.[7] However, their tedious multistep synthesis, low solubility and instability under light and in air have become challenging obstacles to construct them.[8] To address these issues, several strategies have been developed aiming to increase the solubility and kinetically enhance the stability for higher arenes. For example, Introducing the protecting substitutes on the periphery of higher conjugated backbone, such as phenyl, arylthio, fluorine or silylethyne, has been proven as an effective method.[9] Recently, two-Dimensional (2D) construction has been demonstrated as another strategy to stabilize the larger acenes/arenes and a series of zigzag molecules have been prepared to exhibit promising electronic properties.[10] By adopting the rigid terminal/build units such as pyrene, phenanthrene, coronene, several large arenes or N-heteroarenes with single crystals have been prepared.[11] Especially, our group reported a novel stable nonatwistacene through a retro-Diels-Alder process in 2012 as shown in Figure 1.[12] Recently, two longer arenes, decacene and stable decatwistacene (with a large torsion angle of 170 °C), have been reported through either the on-surface generation[13] or introducing stable imide groups.[14] By combining the advantages from a retro-Diels-Alder process (clean reaction) and the cross-conjugated nature of pyrene unit, we firstly reported the synthesis, crystal structure and optical properties of a novel dodecatwistarene (Figure 1).

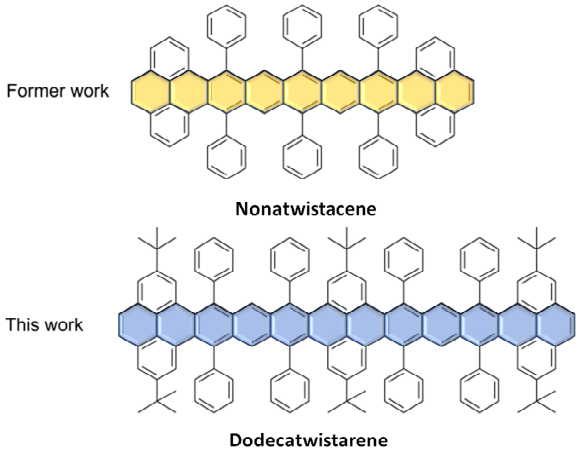

Figure 1. Structures of the reported nonatwistacene and the dodecatwistarene in this work

The synthetic route to dodecatwistarene **4** is shown in scheme 1. Precursor **1** and **2** were synthesized according to the previous reported literatures (the detailed procedures are provided in supporting information S1). [12, 15], [16] The *tert*-butyl groups were purposely introduced on 2, 7 position of pyrene units to increase the solubility of the target molecule **4**. Unexpectedly, rather than obtaining compound **4** as a final product, an intermediate **3** with two carbonyl (C=O) groups as bridges has been separated in 23% yield as a light yellow solid, through a double cycloaddition reaction between as-prepared **2**

[a] Dr. Wangqiao Chen, Dr. Xinxiong Li, Prof. Dr. Qichun Zhang
School of Materials Science and Engineering, Nanyang Technological University (Singapore), 639798, Singapore
E-mail: gczhang@ntu.edu.sg
[b] Dr. Wangqiao Chen, Dr. Ming Liu
Temasek Laboratories @NTU, Nanyang Technological University (Singapore), Research Techno Plaza, 50 Nanyang Drive, 637553 Singapore, E-mail: liuming@ntu.edu.sg
[c] Dr. Guankui Long, Prof. Dr. Mingtao Zhang
Computational Center for Molecular Science, College of Chemistry, Nankai University, Tianjin, 300071, China
[d] Prof. Dr. Naoki Aratani, Prof. Dr. Hiroki Yamada
Graduate School of Materials Science, Nara Institute of Science and Technology (NAIST), 8916-5 Takayama-cholkoma, Japan
[f] Dr. Yongxin Li, Dr. Rakesh Ganguly
Division of Chemistry and Biological Chemistry, School of Physical and Mathematics Science, Nanyang Technological University (Singapore), 637371 Singapore
Wangqiao Chen and Xinxiong Li contribute equally
Supporting information for this article is given via a link at the end of the document.((Please delete this text if not appropriate))

and the *in-situ* generated aryne from compound **1**. The as-prepared intermediate **3** exhibited good solubility in common solvents such as CH_2Cl_2 and $CHCl_3$.

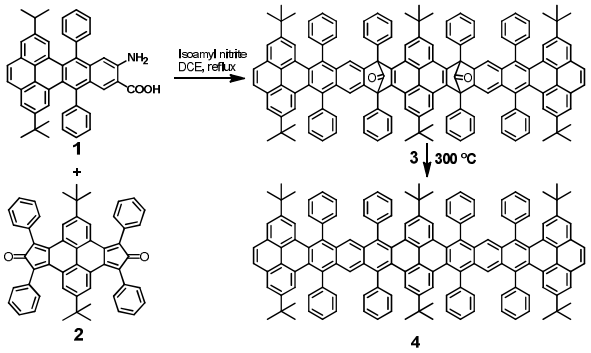

Scheme 1. Synthetic route for **4**

Single crystals of **3** suitable for XRD analysis was grown by slow diffusion of methanol into a $CHCl_3$ solution of **3** within several days (CCDC number: 1848903). As shown in Figure 2, two C=O groups can be clearly observed on both sides of the central pyrene rings. Consequently, the whole molecule **3** exhibits a folded cis-conformation, in which two arms are nearly parallel to each other and perpendicular to the central pyrene ring. Further heat treatment of **3** in the solid state under argon atmosphere at 300 ºC proved to be an effective way to remove C=O bridges and form **4** directly, with a gradual color change from light yellow to orange. The structures of **3** and **4** as well as all other precursors were confirmed by the characterization of ^{1}H NMR, ^{13}C NMR, HRMS as shown in Figure S2-S7. FTIR measurement (Figure S1) indicates that **3** has an apparent strong peak at 1806 cm^{-1}, which indicates the existence of the C=O groups, while the same peak completely disappears in **4**. All other peaks assigned to $–CH_3$ and aromatic –CH groups have almost no difference for both compounds. It is worth to mention that **4** is not stable in CH_2Cl_2 under air for a long time and its color gradually changes from orange to light yellow.

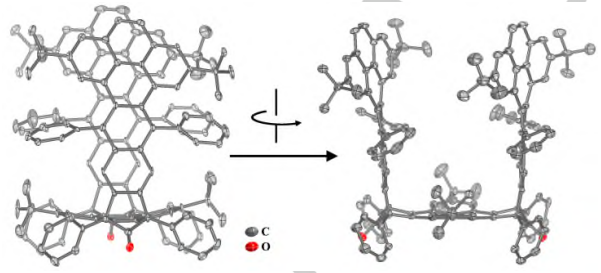

Figure 2. Different views of the crystal structure of **3**. The displacement ellipsoids are draw at 50% probability level, and all hydrogen atoms and solvent molecules are omitted for clarity.

Orange single crystals of **4** (CCDC number: 1848904) as shown in Figure S8 can be obtained through thermal treatment of **3** in diphenyl ether (sealed tube in vacuum) at 300 ºC for 4hrs, followed by gradual cooling. Single crystal XRD analysis reveals that the as-prepared crystal of **4** crystallizes in the triclinic *P*-1 space group with Z value of 2 (S6). The asymmetric unit of 4

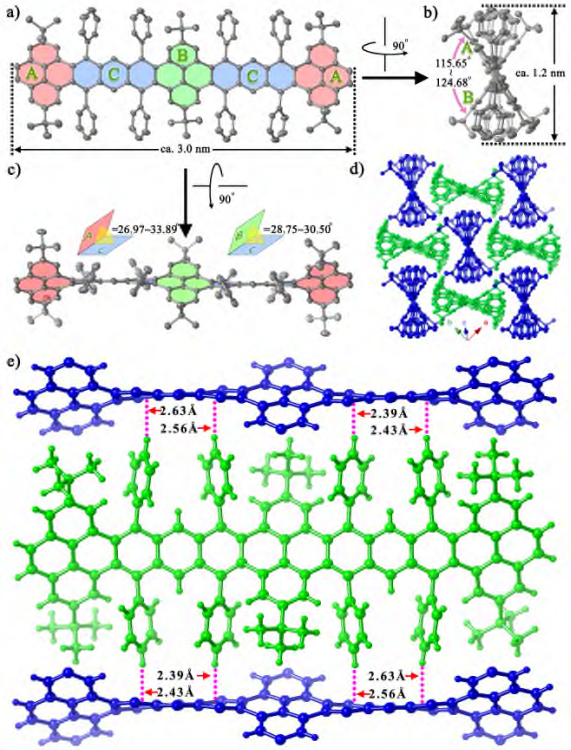

Figure 3. a-c) The molecular structures of **4** in different directions, the displacement ellipsoids are draw at 50% probability level; d) The stacking pattern of molecules in **4**, the two crystallographic unique molecules are marked in different colors; e) The CH-π interactions between two crystallographic unique molecules. The hydrogen atoms in a-d) and part of *tert*-butyl groups and phenyl groups in e) are omitted for clarity.

contains two crystallographic independent fragments of half of the molecular unit (Figure S9). As shown in Figure 3a, the main skeleton of **4** exists in a double-dumbbell fashion and consists of three pyrene units (labeled A, B) and two anthracene species (labeled C). The entire length of the molecule is ~ 3.0 nm and the height is ~1.2 nm (Figure 3b), suggesting that the whole molecule can be considered as a nanobelt. The two end-capping pyrene units in **4** are parallel to each other, and the dihedral angles between the end-capping pyrene units and the center pyrene specie in the two independent molecules are ~ 115.65° and 124.68°, respectively. The two embedded anthracene blocks are also parallel to each other (Figure 3c). The dihedral angles of anthracene units with the end capping pyrene species are ~ 26.97~33.89° in two unique molecules, while the angles between anthracene blocks and the center pyrene units in two unique molecules are in the range of 28.75~30.50°, separately. These results indicate that the main skeleton of **4** does not show good planarity, which is much different from the pyrene-containing N-heteroarene with 12 linearly-fused aromatic six-membered rings reported by us.[17] There is no solvent molecule

in the crystal lattice of **4**, and the two unique molecules in the crystal lattice are stacked in perpendicular to each other (Figure 3d). The stacking style and the steric hindrance arise from the bulky substituting groups around the main skeleton of **4,** which prevents the two adjacent molecules from being close to each other. As a result, there is no π-π interaction between two neighboring molecules. Aside from π-π interaction, XH–π interactions have proven to be prevalent in numerous chemical and biochemical structures.[18] As shown in Figure 3e and Figure S10, the distances between the CH groups on eight phenyl groups and the aromatic backbone of **4** are ~ 2.4 Å and 2.6 Å respectively, suggesting the existence of strong CH–π interactions between the two crystallographic unique molecules, which accounts for their special perpendicular packing model.

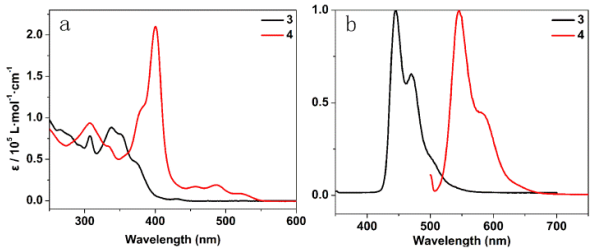

Figure 4. a) UV-Vis absorption (10^{-5} M) and b) fluorescence spectra of **3** and **4** in CH_2Cl_2

The UV-Vis absorption and fluorescence spectra of **3** and **4** were measured in CH_2Cl_2. As shown in Figure 4a, molecule **3** displayed a broad and strong absorption between 250 and 400 nm with the longest absorption λ_{max} at 430 nm while **4** exhibited much bathochromically shifted absorption with the longest λ_{max} at 525 nm (ε = 2.6 × 10^4 L mol^{-1} cm^{-1}) due to the extended conjugation backbone. Overall, similar to the previously reported twisted heptacene by Wudl et al,[19] the λ_{max} of **4** falls between tetracene (475 nm) and pentacene (582 nm). According to the equation of E_g^{opt} = 1240 nm/λ_{onset}, the bandgaps of **3** and **4** are calculated to be 2.79 eV and 2.25 eV, respectively. As shown in Figure 4b, **3** exhibits strong blue fluorescence between 420 nm to 550 nm while **4** displays much red-shifted yellow fluorescence. Interestingly, both **3** and **4** show a similar contour of shoulder peaks for the fluorescence spectra.

Table 1 Physicochemical properties of compounds 3 and 4.

	λ_{onset} (nm)	E_g^{opt} (eV)[a]	E_{ox}^{onset} (V)	HOMO (eV)[b]	LUMO (eV)[c]
3	445	2.79	0.55	–5.35	–2.56
4	550	2.25	0.15	–4.95	–2.70

[a] E_g^{opt} = 1240 nm/λ_{onset} [b] HOMO = HOMO = – (4.80+ E_{ox}^{onset}); [c] LUMO = HOMO + E_g^{opt}

Electrochemical properties of **3** and **4** were measured through Cyclic Voltammetry (CV) in a dry CH_2Cl_2 solution containing 0.1 M tetrabutylammonium hexafluorophosphate (Bu_4NPF_6) and the corresponding curves were recorded as shown in Figure S11. The E_{ox}^{onset} of **3** and **4** were measured to be 0.55 V and 0.15 V in comparison with ferrecene. Hence, their HOMO energy levels were calculated to be –5.35 eV and –4.95 eV, respectively, by taking the empirical equation of HOMO = – (4.80 + E_{ox}^{onset}). Consequently, their LUMO were also calculated to be –2.56 eV and –2.70 eV respectively through the equation of LUMO = HOMO + E_g^{opt}. Therefore, it can be concluded that despite of the increased 0.40 eV for HOMO energy level from **3** to **4** due to its elongated conjugation, the structure transformation has slight effects on their LUMO energy levels. The detailed data are summarized in **Table 1.**

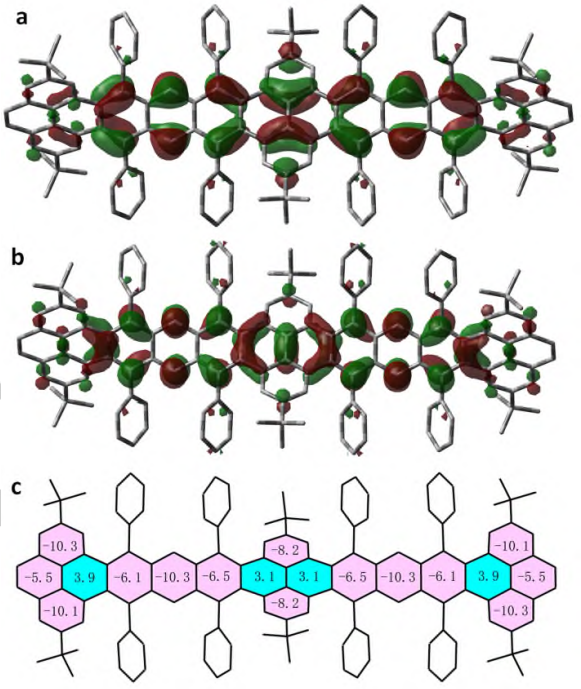

Figure 5. a) HOMO; b) LUMO energy density and c) Nucleus-Independent Chemical Shifts (NICS) calculation for **4**

To gain more insight into the electronic and optical properties of **4**, the optimized geometry was calculated by using DFT calculations (B3LYP/6-31G*, S7), and the subsequent frequency analysis was performed to assure that the optimized structure is the stable state. Based on the calculation results, the wave-function for **4** is stable. Thus, it can conclude that the ground state for this long dodecatwistarene molecule is close-shell singlet rather than open-shell singlet diradical. The HOMO and LUMO orbitals are all delocalized on the polyarene backbone (as shown in Figure 5a and 5b). In addition, the calculated HOMO energy level for **4** (–4.60 eV) is consistent with the experimental value of –4.95 eV, while the calculated bandgap (2.56 eV) matches well with the experimental value of 2.25 eV.

The Nucleus-Independent Chemical Shifts (NICS) calculation was also conducted based on the optimized molecular structure by using the gauge invariant atomic orbital (GIAO) approach at the same B3LYP/6-31G* level. As shown in Figure 5c, the central pyrene units in **4** exhibited a positive NICS(0) value of 3.1, while the values increased to 3.9 on the

side pyrene rings. Similar phenomenon has been observed by Fan et al.[14], which indicates the low aromaticity for the central and terminal pyrene units. On the contrary, other benzene rings in **4** exhibit negative NICS(0) values ranging from –10.3 to –6.1, which further confirms that better aromatic feature exists in the benzene rings other than the pyrene units.

In conclusion, we have successfully synthesized and fully characterized a novel dodecatwistarene for the first time. As far as we know, this is the longest twistarene obtained at present. Single crystal XRD analysis revealed that the large conjugated framework possesses a slightly twisted angle about 30° and two unique dumbbell shaped molecules in the crystal lattice are stacked in perpendicular to each other due to the strong intermolecular CH–π interactions. Our success in preparing dodecatwistarene will provide a direction in preparing higher twistarenes. Further exploring the potential applications of this new material is in progress.

Experimental Section

Synthesis of 4

Method A: 3 (8 mg, 0.0043 mmol) was added into a quartz tube and heated under Argon protection at 300 °C for 2hrs to afford the almost quantitative orange solid of **4**.

Method B: 3 (8 mg, 0.0043 mmol) was added into a quartz tube with 1.0 mL diphenyl ether (degassed) and sealed in high vacuum condition. Then, the tube was put into an oven and heated at 300 °C for 4 hrs. Afterwards, it was cooled down to room temperature and orange crystals precipitated from the solution. ^{1}H NMR (300 MHz, CD_2Cl_2): δ = 8.38 (s, 4H), 8.12 (s, 4H), 7.82 (s, 8H), 7.64 (s, 4H), 7.48-7.35 (m, 40H), 1.09 (s, 36H), 0.65 (s, 18H). ^{13}C NMR (75 MHz, CD_2Cl_2): Due to the low solubility of 4, ^{13}C NMR is not obtained; MALDI-TOF MS: calculated for $C_{140}H_{114}$ + H^+: 1795.8921; found: 1795.8924 (M+ H^+)

Acknowledgements

Q.Z acknowledges financial support from AcRF Tier 1 (RG 111/17, RG 2/17, RG 114/16, RG 8/16) and Tier 2 (MOE 2017-T2-1-021), Singapore. Dr. Liu acknowledges funding support from M4062018.

Keywords: dodecatwistarene • structure • CH–π interactions • synthesis • optical properties

[1] a) M. Bendikov, F. Wudl, D. F. Perepichka, *Chem Rev* **2004**, *104*, 4891-4945; b) J. E. Anthony, *Chem Rev* **2006**, *106*, 5028-5048; c) J. E. Anthony, *Angew Chem Int Ed* **2008**, *47*, 452-483; d) R. A. Pascal, *Chem Rev* **2006**, *106*, 4809-4819; e) M. Rickhaus, M. Mayor, M. Juricek, *Chem Soc Rev* **2016**, *45*, 1542-1556; f) J. Li, S. Chen, Z. Wang, Q. Zhang, *Chem Rec.* **2016**, *16*, 1518-1530.

[2] a) J. E. Anthony, *Angew Chem Int Ed Engl* **2008**, *47*, 452-483; b) J. E. Anthony, *Chem Rev* **2006**, *106*, 5028-5048.

[3] a) J. M. Shi, C. W. Tang, *Appl Phys Lett* **2002**, *80*, 3201-3203; b) M. Kitamura, T. Imada, Y. Arakawa, *Appl Phys Lett* **2003**, *83*, 3410-3412.

[4] a) Y. Shu, Y. F. Lim, Z. Li, B. Purushothaman, R. Hallani, J. E. Kim, S. R. Parkin, G. G. Malliaras, J. E. Anthony, *Chem Sci* **2011**, *2*, 363-368; b) J. Roncali, P. Leriche, P. Blanchard, *Adv Mater* **2014**, *26*, 3821-3838.

[5] Y. W. Son, M. L. Cohen, S. G. Louie, *Nature* **2006**, *444*, 347-349.

[6] L. Bursi, A. Calzolari, S. Corni, E. Molinari, *Acs Photonics* **2014**, *1*, 1049-1058.

[7] a) K. B. Wiberg, *J Org Chem* **1997**, *62*, 5720-5727; b) Z. Wang, P. Gu, G. Liu, H. Yao, Y. Wu, Y. Li, G. Rakesh, J. Zhu, H. Fu, Q. Zhang, *Chem Commun.*, **2017**, *53*, 7772-7775; c) G. Li, H. M. Duong, Z. Zhang, J. Xiao, L. Liu, Y. Zhao, H. Zhang, F. Huo, S. Li, J. Ma, F. Wudl, Q. Zhang, *Chem. Comm.*, **2012**, 48, 5974–5976; d) P.-Y. Gu, Y. Zhao, J.-H. He, J. Zhang, C. Wang, Q.-F. Xu, J.-M. Lu, X. W. Sun, Q. Zhang, *J. Org. Chem.,* **2015**, *80*, 3030-3035; e) J. Li, P. Li, J. Wu, J. Gao, W. Xiong, G. Zhang, Y. Zhao, Q. Zhang, *J. Org. Chem.*, **2014**, *79*, 4438-45

[8] C. Tonshoff, H. F. Bettinger, *Angew Chem Int Edit* **2010**, *49*, 4125-4128.

[9] a) I. Kaur, M. Jazdzyk, N. N. Stein, P. Prusevich, G. P. Miller, *J Am Chem Soc* **2010**, *132*, 1261-+; b) B. Purushothaman, M. Bruzek, S. R. Parkin, A. F. Miller, J. E. Anthony, *Angew Chem Int Edit* **2011**, *50*, 7013-7017.

[10] a) L. Zhang, A. Fonari, Y. Liu, A. L. M. Hoyt, H. Lee, D. Granger, S. Parkin, T. P. Russell, J. E. Anthony, J. L. Bredas, V. Coropceanu, A. L. Briseno, *J Am Chem Soc* **2014**, *136*, 9248-9251; b) G. Zhang, F. Rominger, U. Zschieschang, H. Klauk, M. Mastalerz, *Chem-Eur J* **2016**, *22*, 14840-14845; c) L. Zhang, Y. Cao, N. S. Colella, Y. Liang, J. L. Bredas, K. N. Houk, A. L. Briseno, *Accounts Chem Res* **2015**, *48*, 500-509; d) J. Z. Liu, A. Narita, S. Osella, W. Zhang, D. Schollmeyer, D. Beljonne, X. L. Feng, K. Mullen, *J Am Chem Soc* **2016**, *138*, 2602-2608; e) F. Hinkel, J. Freudenberg, U. H. F. Bunz, *Angew Chem Int Edit* **2016**, *55*, 9830-9832; f) R. Huang, H. Phan, T. S. Herng, P. Hu, W. D. Zeng, S. Q. Dong, S. Das, Y. J. Shen, J. Ding, D. Casanova, J. S. Wu, *J Am Chem Soc* **2016**, *138*, 10323-10330.

[11] a) T. J. Sisto, Y. Zhong, B. Y. Zhang, M. T. Trinh, K. Miyata, X. J. Zhong, X. Y. Zhu, M. L. Steigerwald, F. Ng, C. Nuckolls, *J Am Chem Soc* **2017**, *139*, 5648-5651; b) A. H. Endres, M. Schaffroth, F. Paulus, H. Reiss, H. Wadepohl, F. Rominger, R. Kramer, U. H. F. Bunz, *J Am Chem Soc* **2016**, *138*, 1792-1795; c) E. C. Rudiger, M. Muller, S. Koser, F. Rominger, J. Freudenberg, U. H. F. Bunz, *Chem-Eur J* **2018**, *24*, 1036-1040.

[12] a) J. Xiao, H. M. Duong, Y. Liu, W. X. Shi, L. Ji, G. Li, S. Z. Li, X. W. Liu, J. Ma, F. Wudl, Q. Zhang, *Angew Chem Int Ed* **2012**, *51*, 6094-6098; b) J. Li, Y. Zhao, J. Lu, G. Li, J. Zhang, Y. Zhao, X. Sun, Q. Zhang, *J. Org. Chem.*, **2015**, *80*, 109-113.

[13] J. Kruger, F. Garcia, F. Eisenhut, D. Skidin, J. M. Alonso, E. Guitian, D. Perez, G. Cuniberti, F. Moresco, D. Pena, *Angew Chem Int Ed.* **2017**, *56*, 11945-11948.

[14] W. Fan, T. Winands, N. L. Doltsinis, Y. Li, Z. H. Wang, *Angew Chem Int Ed* **2017**, *56*, 15373-15377.

[15] a) Q. Zhang, J. C. Xiao, Z. Y. Yin, H. M. Duong, F. Qiao, F. Boey, X. A. Hu, H. Zhang, F. Wudl, *Chem-Asian J* **2011**, *6*, 856-862; b) J. Xiao, S. Liu, Y. Liu, L. Ji, X. Liu, H. Zhang, X. Sun, Q. Zhang, *Chem. Asian J.* **2012**, *7*, 561-564; c) J. Xiao, C. D. Malliakas, Y. Liu, F. Zhou, G. Li, H. Su, M. G. Kanatzidis, F. Wudl, Q. Zhang, *Chem. Asian J.* **2012**, *7*, 672-675.

[16] K. Baumgartner, A. L. M. Chincha, A. Dreuw, F. Rominger, M. Mastalerz, *Angew Chem Int Edit* **2016**, *55*, 15594-15598.

[17] P. Y. Gu, Z. R. Wang, G. F. Liu, H. Y. Yao, Z. L. Wang, Y. Li, J. Zhu, S. Z. Li, Q. Zhang, *Chem Mater* **2017**, *29*, 4172-4175.

[18] A. J. Neel, M. J. Hilton, M. S. Sigman, F. D. Toste, *Nature* **2017**, *543*, 637-646.

[19] H. M. Duong, M. Bendikov, D. Steiger, Q. Zhang, G. Sonmez, J. Yamada, F. Wudl, *Org Lett* **2003**, *5*, 4433-4436.

COMMUNICATION

We successfully prepared a novel large dodecatwistarene (**4**) for the first time. Its structure, confirmed by single crystal XRD analysis, indicates that **4** possesses a twisted angle(~ 3o°) and two neighboring molecules in the crystal lattice are perpendicular to each other due to the twisted feature and the strong intermolecular CH–π interactions.

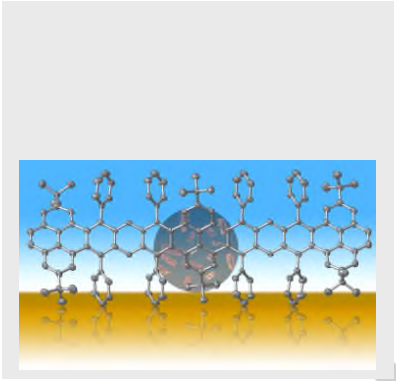

Wangqiao Chen, Xinxiong Li, Guankui Long, Yongxin Li, Rakesh Ganguly, Mingtao Zhang, Naoki Aratani, Hiroko Yamada, Ming Liu and Qichun Zhang**

Page No. – Page No.

Pyrene-Contained Twistarene: Twelve Benzene Rings Fused in One Row